Special Feature: Nanomaterials and Processing

Enhancement of Pressure-free Bonding with Cu Nanoparticles Using Ni Affinity Layers and Ni Alloy Nanoparticles

Toshitaka Ishizaki and Ryota Watanabe

■ABSTRACT∥ Bonding techniques that employ Cu nanoparticles are expected as alternatives to Pb-rich solders that can endure higher temperature than current devices; however, there is a problem in that high bonding temperatures and pressures are necessary for the bonding process. The following three approaches were determined to be effective for enhancement of the shear strengths of bonded Cu plates to be higher than 20 MPa without pressure at 250°C: the use of readily decomposed capping layers on Cu nanoparticles, Ni affinity layers onto bonding interfaces employed to improve adhesion to sintered Cu, and the sintering-assist effects of NiCu or NiSn nanoparticles on Cu nanoparticles. Robust strength was achieved with the developed bonding technique using only base metallic nanoparticles, while the bonding process was similar to that for typical Pb-free solders such as Sn-Cu alloys. This technique is well suited for practical applications because the bonding materials do not contain toxic or expensive elements and the bonding process can be performed by the same method as that for conventional soldering.

■KEYWORDS∥ Pb-free Solder, Sintering, Cu Nanoparticles, Fatty Acids and Amines, Ni Affinity Layer, Ni-alloy Nanoparticles

1. Introduction

It has recently become important to enhance the output density of power devices for effective utilization of energy sources. However, a higher output density leads to an increase in the operating temperature of the device, which results in severe conditions for conventional solder materials.[1] Pb-rich solder is currently the most effective high temperature resistant solder; however, there is a mandatory requirement to remove Pb from electrical devices because of its toxicity.[2] There have been many studies on alternatives to Pb-rich solder, such as Au, Zn and Bi-based alloys; however, there are drawbacks in that Au alloys are expensive, Zn alloys need high temperatures for bonding, and Bi alloys are too brittle and have low thermal conductivities.[3-7]

We have examined a new bonding technique that uses metallic nanoparticles as an alternative to conventional solder because metallic nanoparticles can be sintered at much lower temperatures than the melting points of the bulk metals due to their high surface energy. Therefore, the bonding process can be performed at similar temperatures to those presently used for soldering. There have been many studies on the use of Ag nanoparticles because Ag has the highest thermal conductivity among metals, a high melting point, and is stable enough to obtain nanoparticles without oxidation.[8-11] However, Ag is undesirable for practical use because it is expensive and subject to ion migration.[11] Therefore, we have studied a bonding technique that employs Cu nanoparticles because Cu is inexpensive and also has a high thermal conductivity, a high melting point, and durability against ion migration.

However, there is an important problem with Cu that it is very prone to oxidation, especially on the nanoscale. There have been many reports on the synthesis of Cu nanoparticles capped by polymers because polymers are effective against oxidation and aggregation; however, they cannot be removed easily and the residues inhibit sintering.[12-15] It was previously reported that polyvinyl pyrrolidone (PVP) layers on Cu nanoparticles cannot be decomposed at temperatures up to 400°C and high pressure is necessary to obtain robust sintering strength of Cu nanoparticles, which are severe conditions for die attach materials.[15] It is desirable for practical applications that the bonding process is performed without pressure and at less than 250°C, as with typical

Pb-free solders such as Sn-Cu alloys.[16]

It is necessary to overcome the following challenges to achieve robust strength without pressure and at low temperature:

1. Capping layers should decompose at low temperature,
2. Strong bonded interfaces should be obtained,
3. Strong sintered structures should be obtained.

We have produced high strength bonds without pressure after bonding at 250°C by three approaches: the use of decomposable capping layers (fatty acids and amines) at low temperature,[17] Ni affinity layers onto bonding interfaces employed to improve adhesion to Cu,[18] and sintering-assist effects of Ni alloy particles on Cu nanoparticles.[19,20] This new bonding technique is reported in this paper.

2. Experimental

2. 1 Decomposition Behavior of Cu Nanoparticle Capping Layers

Cu nanoparticles capped by fatty acids and amines were synthesized by changing the alkyl chain length from 10 to 22, and the decomposition behavior of the capping layers were evaluated. 30 mmol of Cu carbonate ($CuCO_3 \cdot Cu(OH)_2 \cdot H_2O$), 30 mmol of fatty acid and 30 mmol of fatty amine were mixed into 300 mL of ethylene glycol ($HO(CH_2)_2OH$). The fatty acids and amines employed were decanoic acid ($C_9H_{19}COOH$) + decyl amine ($C_{10}H_{21}NH_2$), dodecanoic acid ($C_{11}H_{23}COOH$) + dodecyl amine ($C_{12}H_{25}NH_2$), oleic acid ($C_{17}H_{33}COOH$) + oleyl amine ($C_{18}H_{35}NH_2$; OA) and erucic acid ($C_{21}H_{41}COOH$) + erucyl amine ($C_{22}H_{43}NH_2$), respectively. The solution was stirred under a N_2 atmosphere at room temperature for 30 min, then at 110°C for 30 min, and finally heated up to the boiling point and kept for 60 min. The precipitate obtained after cooling was washed with excess hexane and acetone, centrifuged and then dried in a vacuum. The obtained particles are designated as the C10, C12, C18 and C22 Cu nanoparticles according to the alkyl chain length.

The crystal structures of the particles were determined from X-ray diffraction (XRD; RINT-TTR, Rigaku) measurements with a Cu Kα X-ray source operated at 50 kV and 300 mA. Morphological analyses of the particles were conducted using transmission electron microscopy (TEM; JEM-2000EX, JEOL) with an acceleration voltage of 200 kV. The TEM samples were prepared by dropping toluene dispersions of the particles onto a Cu microgrid with an amorphous carbon film. The mean diameter and standard deviation of the particle size distribution were calculated from 200 particles in the TEM micrograph. The thermal decomposition behavior of the capping layers was examined by thermogravimetric and differential thermal analysis (TG-DTA; Thermo Plus TG 8120, Rigaku) from room temperature to 500°C at a rate of 20°C min⁻¹ and with an argon gas flow of 100 mL min⁻¹.

2. 2 Affinity Layers to Cu Nanoparticles

The strengths of bonded Cu plates were evaluated for various metal layers on the Cu plates to determine their affinities for Cu nanoparticles. Cu plates were used for bonding experiments after electrochemical polishing in a mixture of 250 mL phosphoric acid and 10 mL sulfuric acid at 2 V for 5 min. The upper plate was circular (5 mm diameter, 2 mm thick) and the lower plate was rectangular (22×10 mm², 3 mm thick). Metal layers (40 nm thick) of Ni, Cr, Mn or Ti were deposited on the Cu plates by RF sputtering at room temperature. A Cu nanoparticle paste was prepared by adding decanol and α-terpineol to the C10 Cu nanoparticle powder with a C10 Cu nanoparticle s:decanol:α-terpineol weight ratio of 20:1:1. The Cu nanoparticle paste was printed onto the rectangular Cu plate using a metal mask to obtain a printed area and thickness of 5 mm diameter and 0.15 mm, respectively. The circular plates were then placed onto the printed pastes. The samples were bonded by heating without pressure in a hydrogen atmosphere, first at 150°C for 10 min and then for 5 min at 250, 300, 350 or 400°C. The strengths of the bonded samples were then measured by shearing tests at a shear speed of 1 mm min⁻¹ using an advanced materials testing instrument (Instron 5566, Instron) in compression mode. The bonded interface was observed by scanning transmission electron microscopy-energy dispersive X-ray spectroscopic analysis (STEM-EDS; JEM-2010FEF, JEOL) with an acceleration voltage of 200 kV.

2. 3 Sintering-assist by Ni Alloy Nanoparticles

Ni and Ni alloy nanoparticles were synthesized and

added to Cu nanoparticles for pressure-free bonding experiments to evaluate their effect on enhancement of the bonding strengths. For this experiment, Cu nanoparticles were synthesized on a larger scale than that described in Sec. 2.1. First, 120 mmol of Cu carbonate ($CuCO_3 \cdot Cu(OH)_2 \cdot H_2O$), 120 mmol of decanoic acid ($C_9H_{19}COOH$) and 120 mmol of decyl amine ($C_{10}H_{21}NH_2$) were mixed in 600 mL of ethylene glycol ($HO(CH_2)_2OH$). The solution was heated and the particles were then obtained by the same procedure described in Sec. 2.1. The obtained particles are designated as LS C10 Cu nanoparticles.

Ni nanoparticles were synthesized according to the method shown in Ref. (21). First, 7.8 mmol of Ni (II) acetylacetonate ($Ni(C_5H_7O_2)_2$) was added to 54.4 mmol of OA and 6.2 mmol of tri-n-octylphosphine ($P(C_8H_{17})_3$; TOP). The solution was stirred under a N_2 atmosphere at 100°C for 20 min and then at 220°C for 120 min. The colloidal dispersion obtained after cooling was purified by centrifugation and removal of the supernatant solution. The precipitate was then washed successively with excess hexane, acetone and ethanol.

NiCu and NiSn alloy nanoparticles were also synthesized for use as sintering-assists. NiCu nanoparticles were synthesized by stirring a solution of 1.7 mmol Cu (II) acetylacetonate ($Cu(C_5H_7O_2)_2$) and 30 mmol OA under a N_2 atmosphere at 200°C for 60 min. After cooling to room temperature, 0.05-7.2 mmol of Ni (II) chloride ($NiCl_2$) and 2.4 mmol of TOP were added to the solution and stirred under a N_2 atmosphere at 200°C for 60 min. The colloidal dispersion obtained after cooling was centrifuged to remove the supernatant. The precipitate was washed with excess hexane and acetone, centrifuged and then dried in a vacuum. Cu nanoparticles were also synthesized without the addition of $NiCl_2$ for comparison with NiCu nanoparticles. The crystal structure and morphology of the particles were analyzed using the same methods described in Sec. 2.1. The elemental composition of the NiCu nanoparticles was measured using inductively coupled plasma atomic emission spectroscopy (ICP; CIROS-120EOP, Rigaku).

NiSn nanoparticles were synthesized by first preparing Sn nanoparticles as precursors according to the synthesis procedure described in Ref. (22). Briefly, 1.7 mmol of Sn (II) chloride ($SnCl_2$), 32 mmol of OA and 3.6 mmol of tetrabutylammonium borohydride ($C_{16}H_{40}BN$) were mixed into 5 mL of super-dehydrated tetrahydrofuran (C_4H_8O). The solution was stirred under a N_2 atmosphere at 60°C for 60 min. The Sn nanoparticles obtained were collected by centrifugation and washed with excess butanol. The Sn nanoparticles were then mixed into 30 mmol of OA, 0-4.8 mmol of TOP and 1.2 mmol of Ni (II) chloride ($NiCl_2$). The solution was then stirred under a N_2 atmosphere at 200°C for 60 min. The colloidal dispersion obtained after cooling was centrifuged to remove the supernatant. The precipitate was washed with excess hexane and acetone, centrifuged and then dried in vacuum. The crystal structure and morphology of the particles were analyzed using the same methods described in Sec. 2.1.

Cu plates deposited with a 40 nm thick Ni layer were prepared by the same procedure described in Sec. 2.2 for the bonding experiments. Nanoparticle pastes were prepared by adding decanol and α-terpineol to the LS C10 Cu nanoparticle powders and mixed powders consisting of LS C10 Cu nanoparticles (95 wt%) and the Ni or Ni alloy nanoparticles (5 wt%) in a powder:decanol:α-terpineol weight ratio of 20:1:1. The samples were bonded by heating without pressure in a hydrogen atmosphere, first at 200°C for 10 min, and then for 5 min at 250 or 300°C. The strengths of the bonded samples were measured using the same shearing test described in Sec. 2.2. The interfaces of the bonded samples were observed using scanning electron microscopy (SEM; S-3600N, Hitachi) with an acceleration voltage of 15 kV.

3. Results and Discussion

3.1 Decomposition Behavior of Cu Nanoparticle Capping Layers

Figure 1(a) shows XRD patterns of Cu nanoparticles with various alkyl chain length capping layers of fatty acids and amines from C10 to C22. Strong peaks from Cu were observed in all cases, although the patterns for the C18 and C22 Cu nanoparticles also included a weak peak from Cu_2O. The peak from Cu_2O was larger in the pattern for the C22 Cu nanoparticles than that for the C18 Cu nanoparticles. Figures 1(b)-(e) show TEM images of the Cu nanoparticles, where the size of the Cu nanoparticles became smaller as the alkyl chain length of the fatty acid and amine increased. The calculated mean sizes for the C10, C12, C18
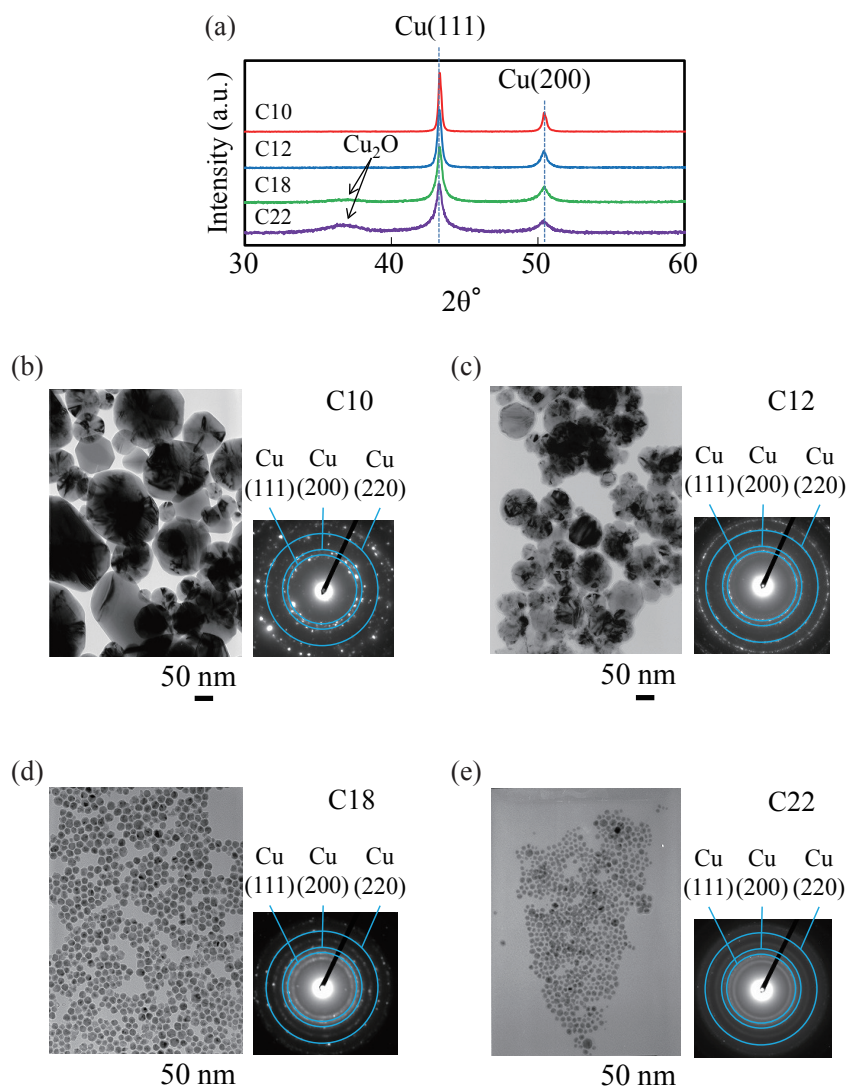
Fig. 1   (a) XRD patterns and (b)-(e) TEM images and diffraction patterns of Cu nanoparticles capped by fatty acids and amines, where the alkyl chain length is from C10 to C22. Broken lines indicate the peaks of Cu (JCPDF card file 04-0836) and arrows indicate the peak of Cu2O (JCPDF card file 35-1091).

and C22 Cu nanoparticles were 92.7, 63.9, 20.0 and 13.3 nm, respectively. The steric hindrance became stronger with the increase of the alkyl chain length, which resulted in smaller particle sizes after synthesis. The C18 and C22 Cu nanoparticles were too small, so that oxidation could not be prevented even with the capping layers, and the volume fraction of Cu_2O on the surfaces of the Cu nanoparticles was large enough to show an XRD peak.

Figures 2(a)-(d) show TG-DTA profiles for the Cu nanoparticles with various alkyl chain lengths of the fatty acid and amine from C10 to C22. All of the profiles had exothermic peaks at temperatures less than 300°C, which is lower than the decomposition temperature of a polymer capping layer.[15] The mass decreases of the C10, C12, C18 and C22 Cu nanoparticles were 0.93, 2.06, 4.24 and 5.01%, respectively. The decrease in mass corresponds to the amount of capping layers on Cu nanoparticles; therefore, it is thought that the amount of capping layers increased as the alkyl chain length increased due to two factors: a decrease in the mean particle diameter led to an increase in the amount of capping layers and an increase in the alkyl chain length led to an increase in the molecular mass. Although the mean particle size increased as the alkyl chain length decreased, the Cu nanoparticles capped by fatty acids and amines with lower alkyl chain lengths had an advantage in terms of sintering due to the lower amount of capping layers.
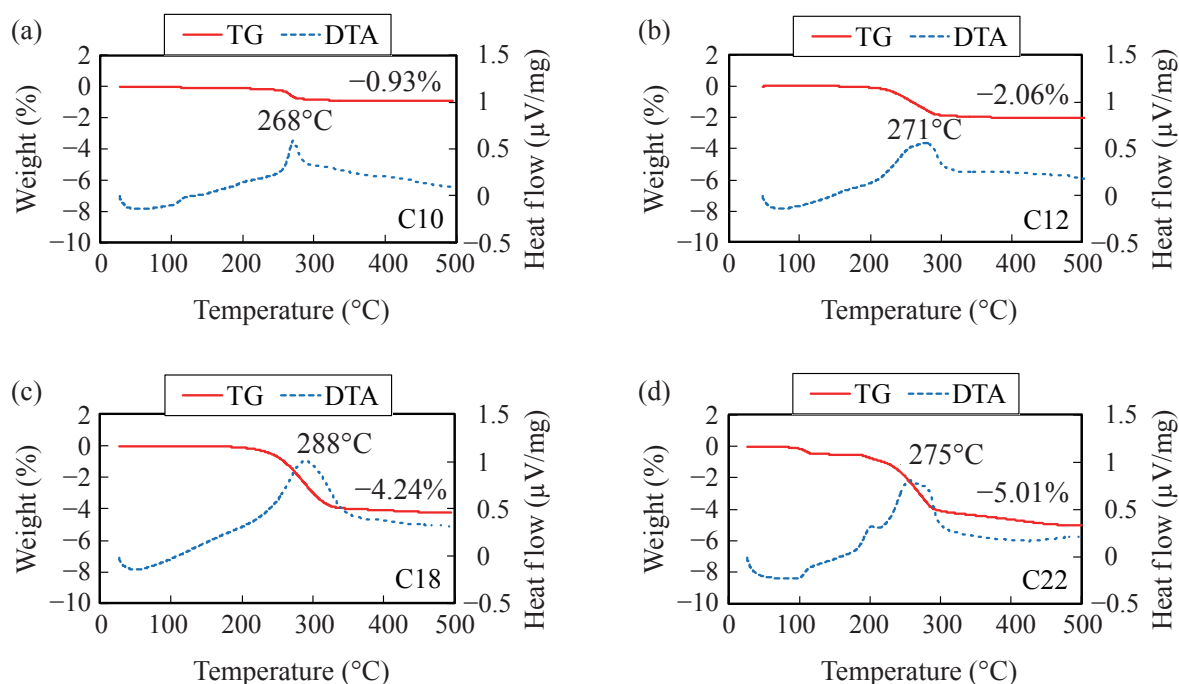
Fig. 2 TG-DTA profiles for Cu nanoparticles capped by fatty acids and amines, where the alkyl chain length is from C10 to C22.

3. 2 Affinity of Metal Layers for Cu Nanoparticles

To evaluate the affinity of metal layers for Cu nanoparticles, the shear strengths of Cu plates with and without metal layers bonded by C10 Cu nanoparticles were measured because the C10 Cu nanoparticles have the lowest amount of capping layers. **Figure 3** shows that the bonded Cu plates with Ni layers exhibited the highest strength, while the Cu plates without metal layers or with Ti, Mn and Cr layers were easily sheared apart. When no metal layer was deposited onto the Cu plates, the connection between the Cu plates and sintered Cu nanoparticles was weak without pressure, so that the shear strength was very weak. In the cases where Ti, Mn and Cr layers were deposited, the surfaces formed a stable oxidation layer that could not be reduced, even with hydrogen, because the standard free energies of oxide formation for Ti, Mn and Cr are much lower than those for other metals. On the other hand, Ni oxides are more easily reduced than oxides of Ti, Mn and Cr; therefore, the Ni oxides were readily reduced in the hydrogen atmosphere. In addition, Ni-Cu alloy is well known as a complete solid solution system, so that there is favorable affinity between Cu and Ni to assist in the formation of a strong bond. The interface of the Cu plates with Ni affinity layers
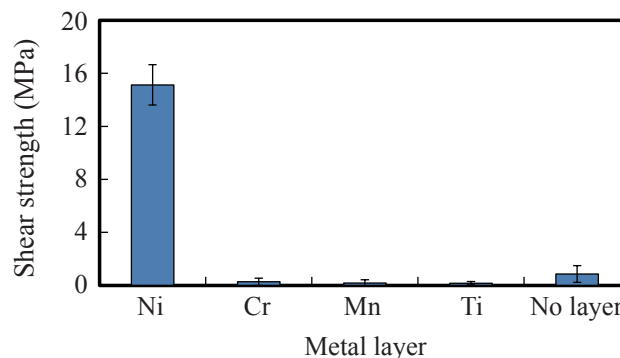

Fig. 3 Effects of metal affinity layers on the shear strengths of Cu plates bonded with C10 Cu nanoparticles at 300°C.

bonded with C10 Cu nanoparticles was observed using STEM-EDS, as shown in **Fig. 4**. These results indicate that a thin layer of Cu is spread along the Ni surface, which results in a strong connection. The mechanism by which the Ni layer improves the affinity with Cu nanoparticles was studied in another paper.[23]

3. 3 Sintering-assist Effect of Ni Alloy Nanoparticles

The previous section shows that Ni layers can enhance the affinity with sintered Cu to obtain high shear strength for Cu plates bonded with

Cu nanoparticles. However, this strength is not large enough compared with that achieved with conventional solders.[6] In addition, the bonding temperature is higher than that for Sn-based solders. Thus, the sintered structures must be strengthened much more because micropores remained in the sintered Cu, as shown in Fig. 4.

Ni exhibited favorable affinity to Cu; therefore, Ni nanoparticles were added to the LS C10 Cu nanoparticle paste for bonding experiments to evaluate whether Ni nanoparticles can enhance the bonding strengths. **Figure 5** shows an XRD pattern and TEM image of the synthesized Ni nanoparticles. Only peaks from Ni were observed in the XRD pattern and the particle size estimated from the TEM image was 14 nm. The shear strengths of the Cu plates with Ni layers bonded using only Cu nanoparticles or the Cu-5 wt% Ni mixed nanoparticles as bonding materials are shown in **Fig. 6**. The shear strengths were almost the same at bonding temperatures of 250 and 300°C, with and without the Ni nanoparticles. Therefore, the Ni nanoparticles did not enhance the shear strength. The sintering temperature is dependent on the melting point; therefore, it is presumed that the Ni nanoparticles cannot be sintered sufficiently, and sintered Cu cannot be strengthened by the addition of the Ni nanoparticles at these temperatures because the melting point of Ni (1455°C) is higher than that of Cu (1085°C).

Thus, Ni nanoparticles should be alloyed with a metal with a melting point lower than Ni to decrease the sintering temperature. NiCu nanoparticles were synthesized because the melting point of Cu is lower than that of Ni. **Figures 7** and **8** show XRD patterns and TEM images of NiCu and Cu nanoparticles synthesized using the same procedure described in

Sec. 2.3. The XRD pattern for the Cu nanoparticles shows a strong peak from Cu and a weak peak from Cu_2O, while those for the NiCu nanoparticles have strong peaks between the expected positions of Cu and Ni, with a shift to higher angle with an increase in the amount of $NiCl_2$. This indicates that the alloying of Ni with Cu decreases the size of the crystal lattice. The Cu and Ni atomic ratios in NiCu nanoparticles estimated from ICP analyses were almost consistent with the feed ratio of Cu and Ni salts in the mother liquor, as shown in **Table 1**. The magnified XRD pattern for
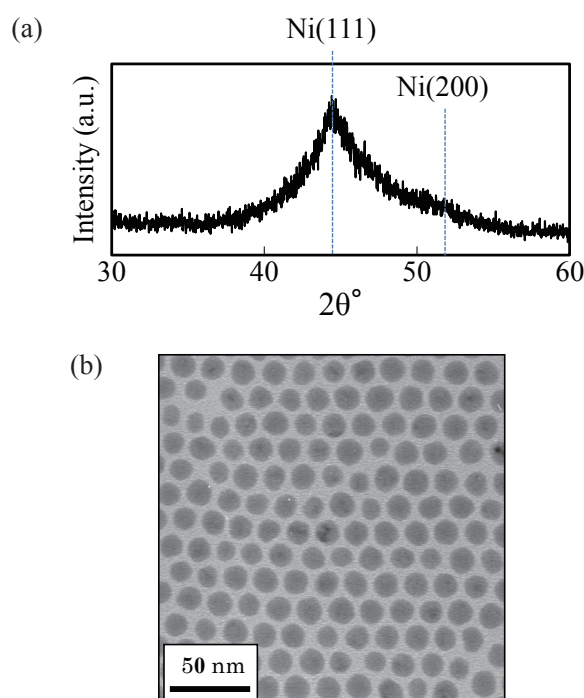

Fig. 5   (a) XRD pattern and (b) TEM image of the Ni nanoparticles. Broken line indicates the peaks of Ni (JCPDF card file 04-0850).
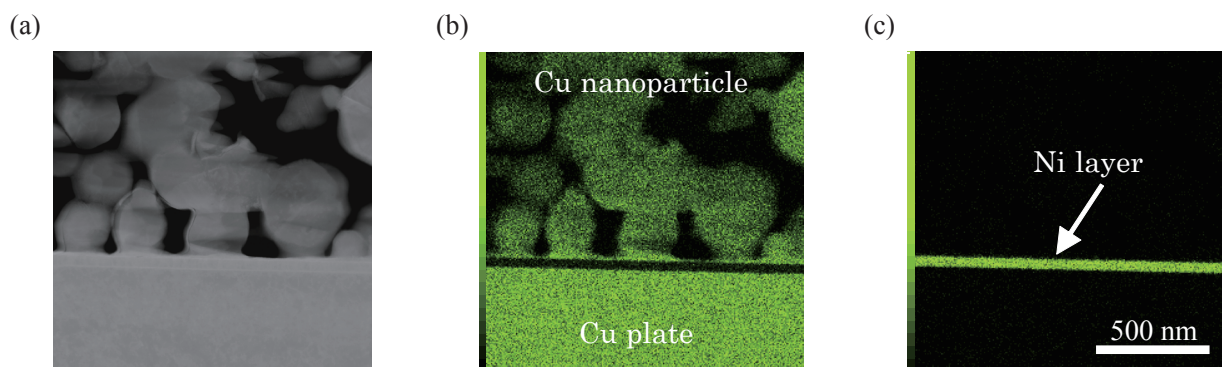

Fig. 4   (a) STEM image and EDS atomic maps for (b) Cu and (c) Ni at the interface of Cu plates with Ni layers bonded with C10 Cu nanoparticles at 300°C.

NiCu nanoparticles produced with 0.05 mmol of $NiCl_2$ had a weak peak from Cu_2O, as did that for the Cu nanoparticles; however, no weak peak from Cu_2O was observed for the NiCu nanoparticles produced with $NiCl_2$ amounts greater than 0.05 mmol, as shown in Fig. 7(b). This result indicates that the oxidation stability is improved by the addition of Ni. Table 1 summarizes the particle sizes estimated from TEM images of the NiCu and Cu nanoparticles shown in Fig. 8. The particle size became larger from 9 to 16 nm
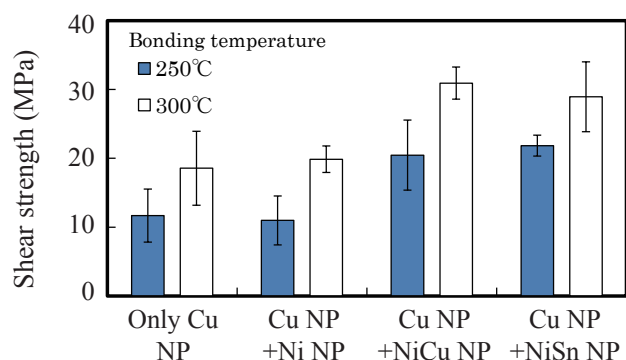
as the Ni ratio was increased, due to the growth of the nanoparticles during the Ni alloying reaction. NiCu nanoparticles prepared with 3.6 mmol of $NiCl_2$ were added to the LS C10 Cu nanoparticle paste for bonding experiments to evaluate whether NiCu nanoparticles can enhance the shear strength. Figure 6 shows that the addition of NiCu nanoparticles significantly enhanced the shear strengths at both bonding temperatures of 250 and 300°C.

Ni nanoparticles were also alloyed with Sn because Sn also has a lower melting point than that of Ni. Syntheses of NiSn nanoparticles were carried out with the molar ratio of TOP to OA increased from 0 to 0.16, while the amount of OA (30 mmol) was kept constant. All XRD patterns for the particles obtained had peaks from Ni_3Sn_2 without oxidation, as shown in **Fig. 9**. **Figure 10** shows TEM images of the NiSn nanoparticles. Polydisperse and irregularly shaped nanoparticles were observed when TOP was not added. On the other hand, the particle size decreased from 16 to 15 nm and the particle shape became monodisperse and cubic as the molar ratio of TOP to OA was increased to 0.08. Thus, the increase in the amount of TOP led to narrower size distributions and greater numbers of cube-shaped NiSn nanoparticles. However, the particle shape changed to polydisperse
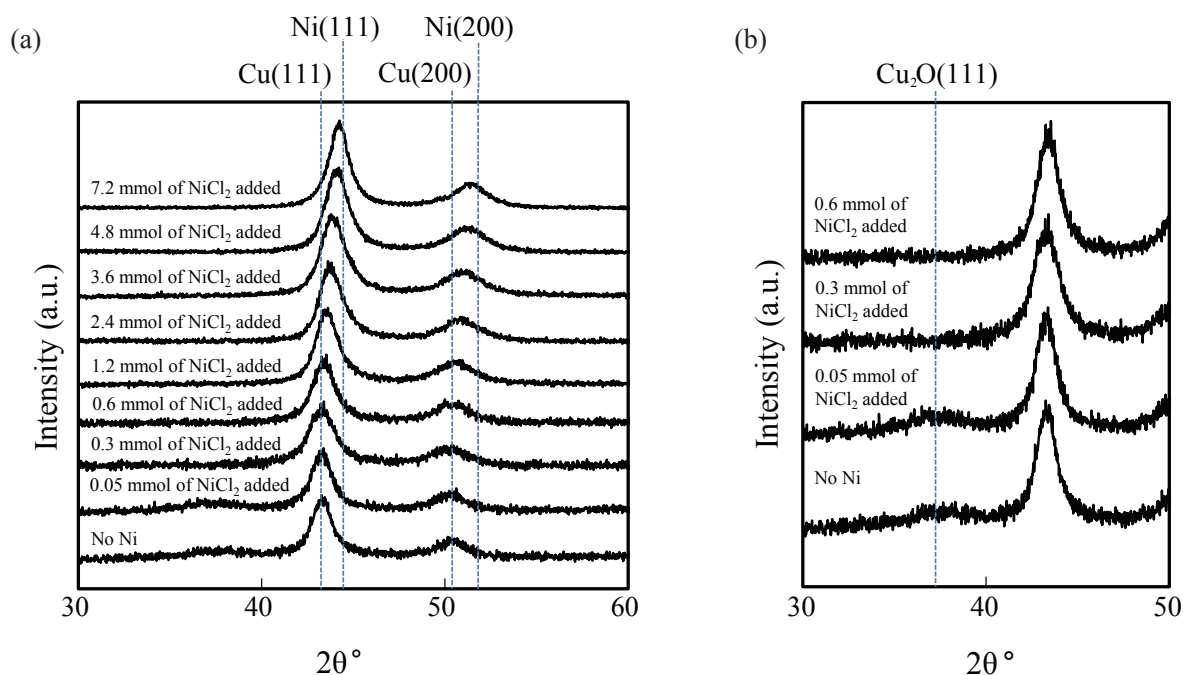

Fig. 6   Shear strengths of Cu plates with Ni affinity layers bonded with only the LS C10 Cu nanoparticles, and with LS C10 Cu-5 wt% Ni, NiCu or NiSn mixed nanoparticles at 250 and 300°C.

Fig. 7   (a) XRD patterns for Cu nanoparticles and NiCu nanoparticles with 0.05-7.2 mmol of added $NiCl_2$. (b) Magnified XRD patterns for Cu nanoparticles and NiCu nanoparticles with 0.05-0.6 mmol of added $NiCl_2$. Broken lines indicate the peaks of Cu (JCPDF card file 04-0836), Ni (JCPDF card file 04-0850) and Cu_2O (JCPDF card file 35-1091).
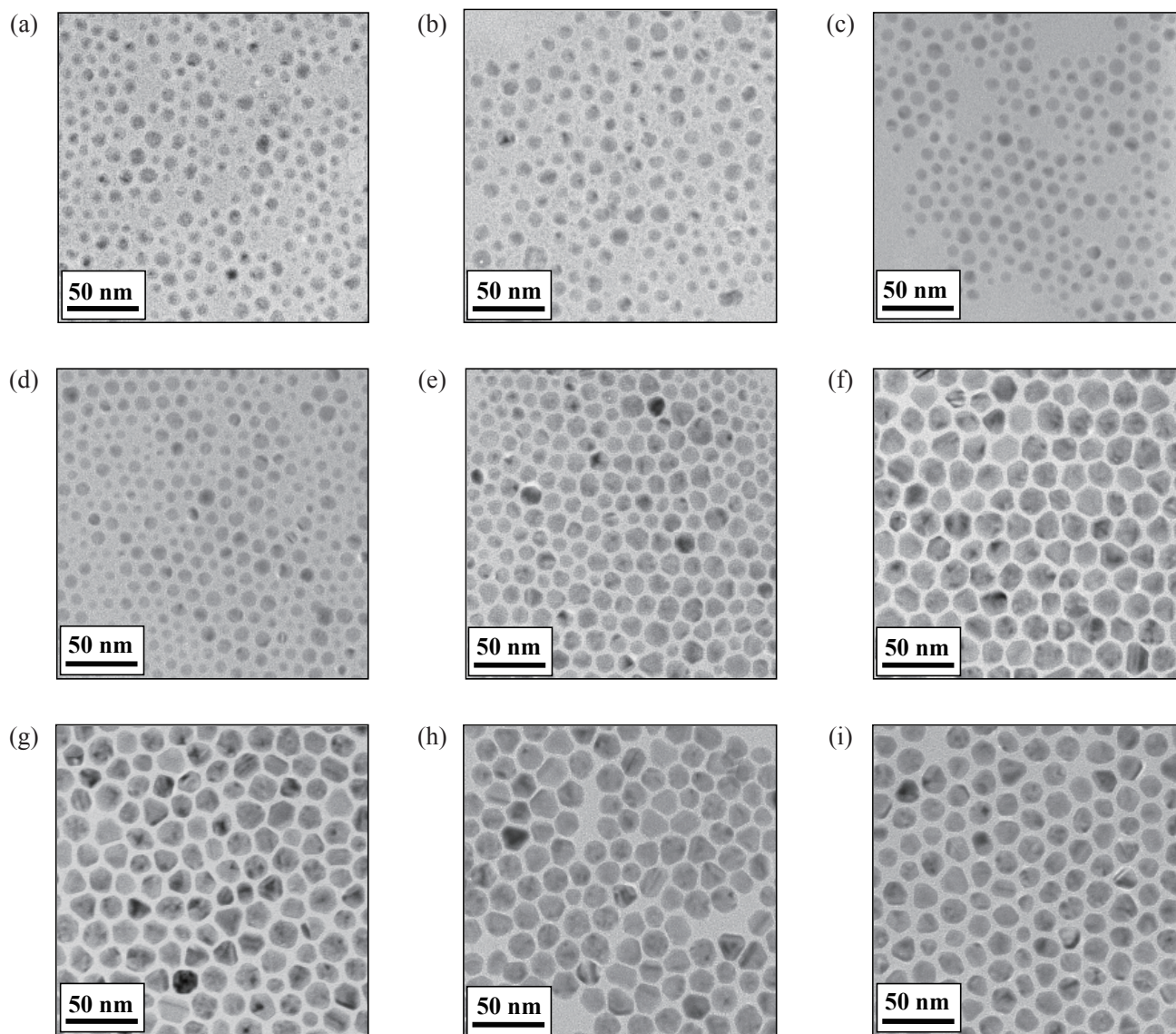
Fig. 8　TEM images of (a) Cu nanoparticles, and NiCu nanoparticles produced with (b) 0.05, (c) 0.3, (d) 0.6, (e) 1.2, (f) 2.4, (g) 3.6, (h) 4.8, and (i) 7.2 mmol of added NiCl$_2$.

and irregular again when the molar ratio of TOP to OA was larger than 0.12. Carenco et al. reported that the particle shape and size is strongly dependent on the molar ratio of TOP to OA.[21] The present results indicate that the optimum ratio of TOP to OA to obtain monodisperse and cube-shaped NiSn nanoparticles is 0.08. NiSn nanoparticles with a molar TOP to OA ratio of 0.08 were also added to the LS C10 Cu nanoparticle paste for bonding experiments to evaluate whether NiSn nanoparticles could enhance the shear strength as well as NiCu nanoparticles. Figure 6 shows that the shear strength was also enhanced by the addition of NiSn nanoparticles at both bonding temperatures of 250 and 300°C.

SEM observations of the interfaces between Cu plates bonded by the paste consisting of only Cu nanoparticles and Cu-5 wt% Ni, NiCu and NiSn mixed nanoparticles at 250°C were conducted (**Fig. 11**) to investigate the relationship between the shear strength and the sintered structures. Figures 11(a) and (b) show that the sintered structures obtained with only the LS C10 Cu nanoparticles and the LS C10 Cu-5 wt% Ni mixed nanoparticles contained a larger number of microvoids, whereas Figs. 11(c) and (d) show that more densely sintered structures were formed by the addition of NiCu or NiSn nanoparticles. These sintered structures were consistent with the observed bonding strengths. It is presumed that Ni nanoparticles

Table 1 Summary of Cu and Ni compositions estimated from ICP measurements, and the average diameter of Cu nanoparticles estimated from TEM measurements.

| Entry | Atomic ratio (%) | | | | |
| | Mother liquor | | ICP | | |
	Cu	Ni	Cu	Ni	D^a (nm)
Cu nanoparticles	100	0			9.3
NiCu nanoparticles with NiCl$_2$ of 0.05 mmol	97	2.9	97	3.3	9.2
NiCu nanoparticles with NiCl$_2$ of 0.3 mmol	85	15	81	19	8.6
NiCu nanoparticles with NiCl$_2$ of 0.6 mmol	74	26	68	32	8.6
NiCu nanoparticles with NiCl$_2$ of 1.2 mmol	59	41	55	45	10.0
NiCu nanoparticles with NiCl$_2$ of 2.4 mmol	41	59	39	61	15.9
NiCu nanoparticles with NiCl$_2$ of 3.6 mmol	32	68	29	71	15.1
NiCu nanoparticles with NiCl$_2$ of 4.8 mmol	26	74	23	77	16.5
NiCu nanoparticles with NiCl$_2$ of 7.2 mmol	19	81	17	83	14.8

[a] Average particle diameter estimated from TEM images.

did not assist sintering of the Cu nanoparticles due to their high melting point, while the NiCu and NiSn nanoparticles enhanced sintering of the Cu structures, even at 250°C, due to alloying between Ni and the metals with lower melting points than Ni.

It is noteworthy that the shear strength of Cu plates with Ni affinity layers bonded without pressure by the paste consisting of Cu and NiCu or NiSn nanoparticles was higher than 20 MPa, even at 250°C, which is the same temperature applied for conventional Sn-Cu alloy solders. This strength is almost the same level as that achieved with Pb-rich solder, even though the process temperature is much lower than that used for Pb-rich solder.[6] These alternative solder materials do not contain toxic elements or noble metals; therefore, this bonding technique can be used to both reduce the environmental load and lower material costs. Thus, the proposed bonding technique with the use of Cu and Ni-alloy mixed nanoparticles and the application of Ni affinity layers onto the bonding interfaces is
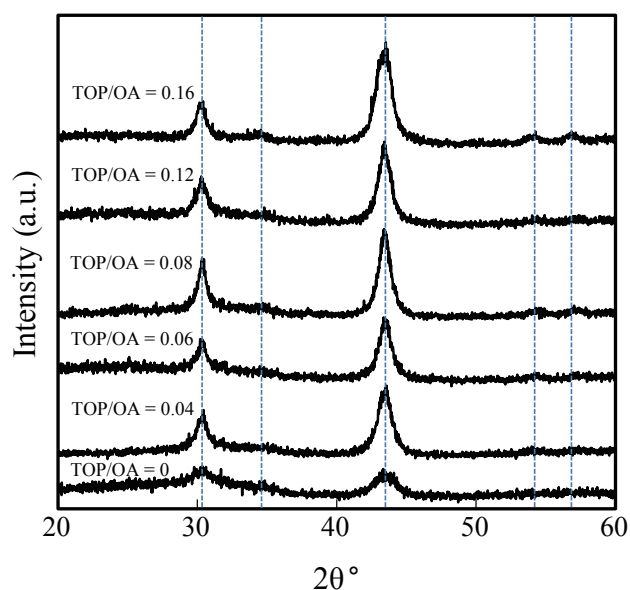

Fig. 9 XRD patterns for NiSn nanoparticles synthesized with TOP to OA molar ratios of 0, 0.04, 0.06, 0.08, 0.12 and 0.16. Broken lines indicate the peaks of Ni$_3$Sn$_2$ (JCPDF card file 07-0256).
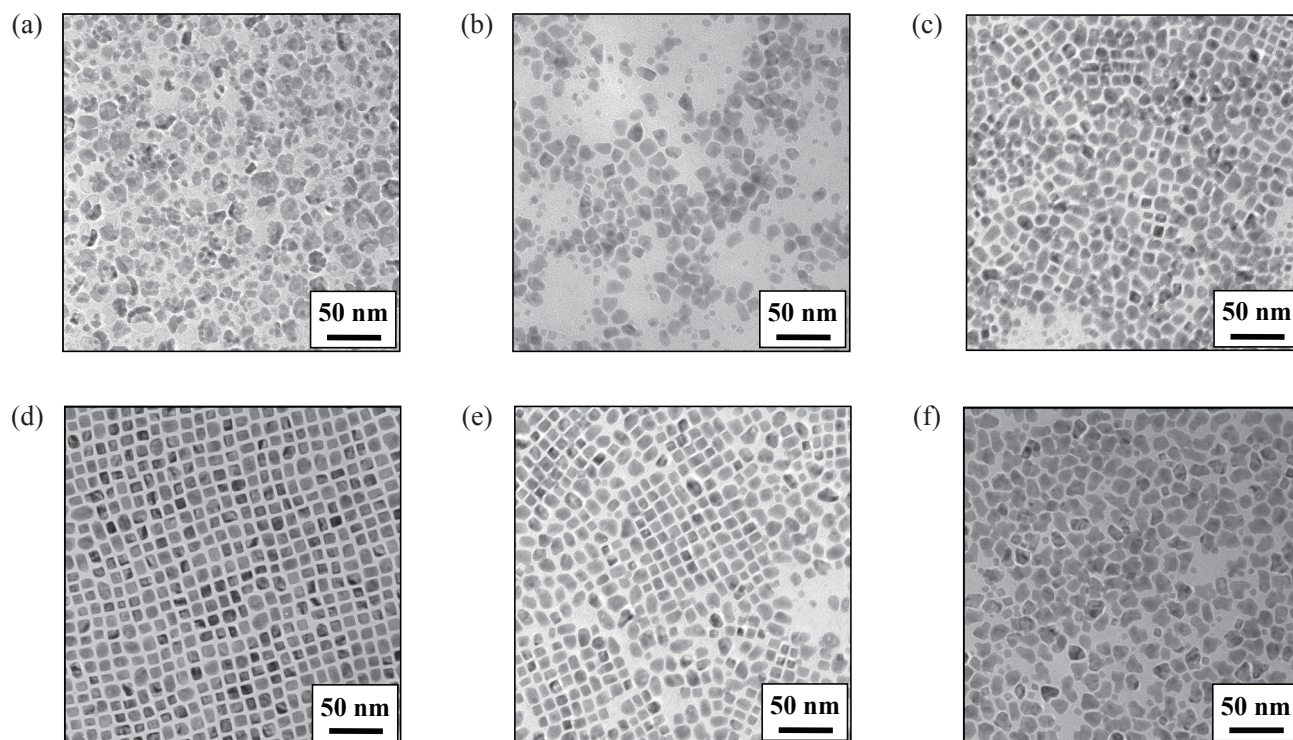
Fig. 10 TEM images of NiSn nanoparticles synthesized with TOP to OA molar ratios of (a) 0, (b) 0.04, (c) 0.06, (d) 0.08, (e) 0.12 and (f) 0.16.
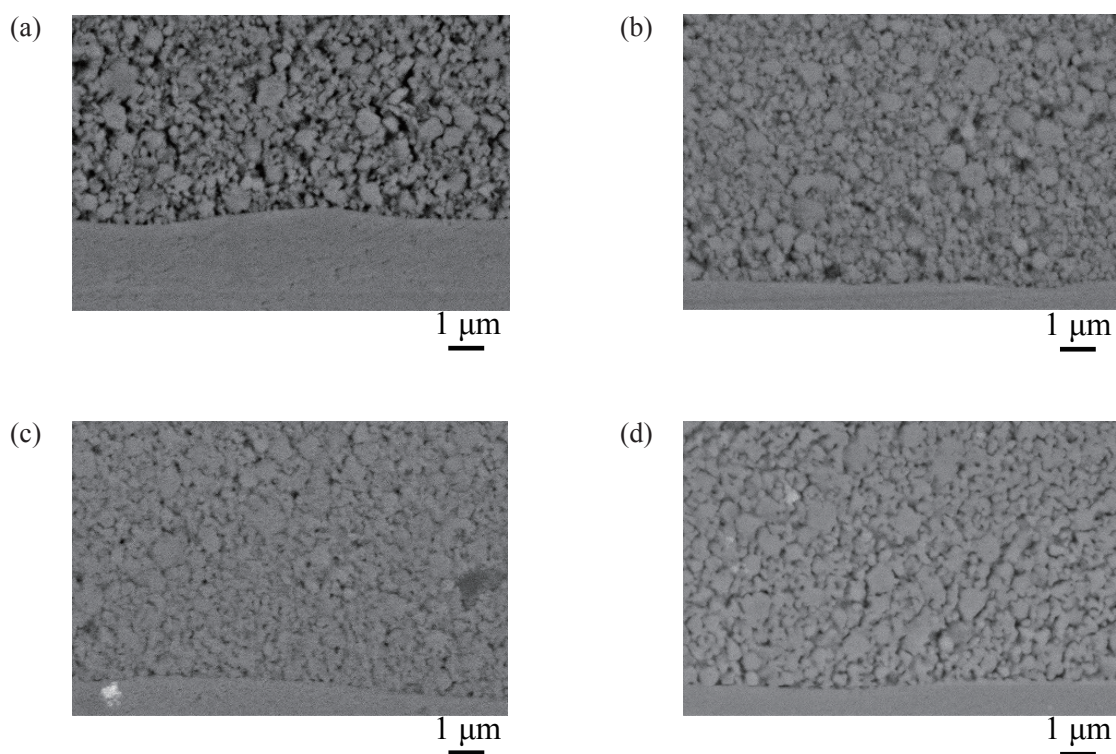

Fig. 11 SEM images of the interfaces of Cu plates bonded with (a) LS C10 Cu nanoparticles, and with (b) LS C10 Cu-5 wt% Ni, (c) NiCu or (d) NiSn mixed nanoparticles at 250°C.

considered to have excellent potential as an alternative to Pb-rich solder that can be carried out using the same process as used for Sn-Cu alloy solders.

4. Conclusion

This study revealed that robustly bonded Cu plates could be obtained even at 250°C by sintering of Cu nanoparticles (and the addition of NiCu or NiSn nanoparticles) capped by fatty acids and amines, and with application of Ni affinity layers onto the Cu plates. The capping layers consist of fatty acids and amines on Cu nanoparticles that can be decomposed even in an inert atmosphere at lower temperatures than the decomposition temperature of typical polymer capping layer. The Ni affinity layers deposited onto Cu plates prior to bonding significantly enhanced adhesion to the sintered Cu nanoparticles, while Ti, Mn and Cr layers did not show a similar effect. The sintered Cu nanoparticles could be strengthened by Ni nanoparticles alloyed with metals that have lower melting points than Ni (NiCu, NiSn). This new bonding technique is well suited for practical use because significant bonding strength can be achieved without the use of toxic and expensive materials, and without the need for pressure at low temperature, as with the conventional Pb-free soldering process.

References

(1) Chin, H. S., Cheong, K. Y. and Ismail, A. B., "A Review on Die Attach Materials for SiC-based High Temperature Power Devices", *Metal. Mater. Trans. B*, Vol. 41B (2010), pp. 824-832.

(2) Desmarest, S. G., "Reliability of Pb-free Solders for Harsh Environment Electronic Assemblies", *Mater. Sci. Tech.*, Vol. 28, No. 3 (2012), pp. 257-273.

(3) Tsai, J. Y., Chang, C. W., Shieh, Y. C., Hu, Y. C. and Kao, C. R., "Controlling the Microstructures from the Gold-Tin Reaction", *J. Electron. Mater.*, Vol. 34, No. 2 (2005), pp. 182-187.

(4) Song, H. G., Ahn, J. P. and Morris, J. W. Jr., "The Microstructure of Eutectic Au-Sn Solder Bumps on Cu/electroless Ni/Au", *J. Electron. Mater.*, Vol. 30, No. 9 (2001), pp. 1083-1087.

(5) Yamada, Y., Takaku, Y., Yagi, Y., Nakagawa, I., Atsumi, T., Shirai, M., Ohnuma, I. and Ishida, K., "Reliability of Wire-bonding and Solder Joint for High Temperature Operation of Power Semiconductor Device", *Microelectron. Reliab.*, Vol. 47 (2007), pp. 2147-2151.

(6) Kim, S., Kim, K.-S., Kim, S.-S., Suganuma, K. and Izuta, G., "Improving the Reliability of Si Die Attachment with Zn-Sn-based High-temperature Pb-free Solder Using a TiN Diffusion Barrier", *J. Electron. Mater.*, Vol. 38, No. 12 (2009), pp. 2668-2675.

(7) Haque, A., Lim, B. H., Haseeb, A. S. M. A. and Masjuk, H. H., "Die Attach Properties of Zn-Al-Mg-Ga Based High-temperature Lead-free Solder on Cu Lead-frame", *J. Mater. Sci. : Mater. Electron.*, Vol. 23 (2012), pp. 115-123.

(8) Siow, K. S., "Mechanical Properties of Nano-silver Joints as Die Attach Materials", *J. Alloys Compd.*, Vol. 514 (2012), pp. 6-19.

(9) Siow, K. S., "Are Sintered Silver Joints Ready for Use as Interconnect Material in Microelectronic Packaging?", *J. Electron. Mater.*, Vol. 43, No. 4 (2014), pp. 947-961.

(10) Khazaka, R., Mendizabal, L. and Henry, D., "Review on Joint Shear Strength of Nano-silver Paste and Its Long-term High Temperature Reliability", *J. Electron. Mater.*, Vol. 43, No. 7 (2014), pp. 2459-2466.

(11) Peng, P., Hu, A., Gerlich, A. P., Zou, G., Liu, L. and Zhou, N., "Joining of Silver Nanomaterials as Low Temperatures: Processes, Properties, and Applications", *ACS Appl. Mater. Interfaces*, Vol. 7 (2015), pp. 12597-12618.

(12) Jeong, S., Woo, K., Kim, D., Lim, S., Kim, J. S., Shin, H., Xia, Y. and Moon, J., "Controlling the Thickness of the Surface Oxide Layer on Cu Nanoparticles for the Fabrication of Conductive Structures by Ink-jet Printing", *Adv. Funct. Mater.*, Vol. 18 (2008), pp. 679-686.

(13) Tomonari, M., Ida, K., Yamashita, H. and Yonezawa, T., "Size-controlled Oxidation-resistant Copper Fine Particles Covered by Biopolymer Nanoskin", *J. Nanosci. Nanotech.*, Vol. 8, No. 5 (2008), pp. 2468-2471.

(14) Choi, C. S., Jo, Y. H., Kim, M. G. and Lee, H. M., "Control of Chemical Kinetics for Sub-10 nm Cu Nanoparticles to Fabricate Highly Conductive Ink below 150°C", *Nanotechnology*, Vol. 23 (2012), 065601.

(15) Yan, J., Zou, G., Hu, A. and Zhou, Y. N., "Preparation of PVP Coated Cu NPs and the Application for Low-temperature Bonding", *J. Mater. Chem.*, Vol. 21 (2011), pp. 15981-15986.

(16) Gao, Y., Hui, J., Sun, X., Zhao, F., Zhao, J., Cheng, C., Luo, Z. and Wang, L., "Role of Zinc on Shear Property Evolution between Sn-0.7Cu Solder and Joints", *Procedia Eng.*, Vol. 16 (2011), pp. 807-811.

(17) Ishizaki, T. and Watanabe, R., "A New One-pot

Method for the Synthesis of Cu Nanoparticles for Low Temperature Bonding", *J. Mater. Chem.*, Vol. 22 (2012), pp. 25198-25206.

(18) Ishizaki, T., Akedo, T., Satoh, T. and Watanabe, R., "Pressure-free Bonding of Metallic Plates with Ni Affinity Layers Using Cu Nanoparticles", *J. Electron. Mater.*, Vol. 43, No. 3 (2014), pp. 774-779.

(19) Watanabe, R. and Ishizaki, T., "Enhancement of Pressure-free Bonding with Cu Particles by the Addition of Cu-Ni Alloy Nanoparticles", *J. Mater. Chem. C*, Vol. 2 (2014), pp. 3542-3548.

(20) Watanabe, R. and Ishizaki, T., "High-strength Pressure-free Bonding Using Cu and Ni-Sn Nanoparticles", *Part. Part. Syst. Charact.*, Vol. 31 (2014), pp. 699-705.

(21) Carenco, S., Boissière, C., Nicole, L., Sanchez, C., Floch, P. L. and Mézailles, L., "Controlled Design of Size-tunable Monodisperse Nickel Nanoparticles", *Chem. Mater.*, Vol. 22 (2010), pp. 1340-1349.

(22) Watanabe, R. and Ishizaki, T., "Size- and Shape-controlled Syntheses of Colloidal Sn, Te, and Bi Nanocrystals", *Bull. Chem. Soc. Jpn.*, Vol. 86, No. 5 (2013), pp. 642-650.

(23) Satoh, T., Akedo, K. and Ishizaki, T., "X-ray Photoelectron Spectroscopic Study of the Formation of Cu/Ni Interface Mediated by Oxide Phase", *J. Alloys Compd.*, Vol. 582 (2014), pp. 403-407.

Figs. 1 and 2
Reprinted from J. Mater. Chem., Vol. 22 (2012), pp. 25198-25206, Ishizaki, T. and Watanabe, R., "A New One-pot Method for the Synthesis of Cu Nanoparticles for Low Temperature Boding", © 2012 The Royal Society of Chemistry.

Figs. 3 and 4
Reprinted from J. Electron. Mater., Vol. 43 (2014), pp. 774-779, Ishizaki, T., Akedo, K., Satoh, T. and Watanabe, R., "Pressure-free Bonding of Metallic Plates with Ni Affinity Layers Using Cu Nanoparticles", © 2014 TMS, with permission from Springer.

Figs. 5, 7, 8 and Table 1
Reprinted from J. Mater. Chem. C, Vol. 2 (2014), pp. 3542-3548, Watanabe, R. and Ishizaki, T., "Enhancement of Pressure-free Bonding with Cu Particles by the Addition of Cu-Ni Alloy Nanoparticles", © 2014 The Royal Society of Chemistry.

Figs. 9 and 10
Reprinted from Part. Part. Syst. Charact., Vol. 31 (2014), pp. 699-705, Watanabe, R. and Ishizaki, T., "High-strength Pressure-free Boding Using Cu and Ni-Sn Nanoparticles", © 2014 Wiley-VCH Verlag GmBH & Co., with permission from John Wiley and Sons.

Toshitaka Ishizaki
 Research Fields:
  - Nanoparticle
  - Colloid
  - Joint Technology
 Academic Degree: Dr.Eng.
 Academic Societies:
  - The Chemical Society of Japan
  - The Society of Nano Science and Technology

Ryota Watanabe
 Research Field:
  - Polymer Chemistry
 Academic Degree: Dr.Eng.
 Academic Societies:
  - The Chemical Society of Japan
  - The Society of Polymer Science
  - Catalysis Society of Japan
 Award:
  - CSJ Presentation Award, The Chemical Society of Japan, 2015
 Present Affilication: National Institute of Advanced Industrial Science and Technology